UDC 629.7.015.4

Mosunov V. A., Ryabykina R. V.,
Smyslov V. I., Frolov A. V.

Experience of computational research on the flutter of an unmanned aerial vehicle

The paper focuses on the sequence of computational and experimental investigations on the flutter. We set the initial data for the unmanned aerial vehicle and built the mathematical models. Furthermore, we did parametric analysis of symmetric and antisymmetric flutter shapes of the wings and the tail, studied the aerodynamics effect on the body of the vehicle, gave the examples of the calculation data on the base of KS-M and *MSC.Nastran* software.

Keywords: flutter, unmanned aerial vehicle, computational and experimental investigations, symmetric model, antisymmetric model.

Introduction

Flutter is dangerous self-excited vibration of the unmanned aerial vehicle (UAV) caused by interaction between the elastic structure and the airflow. As soon as such self-excited vibrations reach or even exceed the stability limit in any flight regime, they may cause destruction of the UAV structure or malfunction of its systems. The UAV flight safety assessment regarding flutter is the ultimate goal of computational and experimental investigations including series of parameter computations, ground tests of individual units and structure of the UAV as a whole [1, 2].

Based on computational studies, we should note that mass-elastic dynamic models need to be updated according to ground test results. The use of various software packages may contribute to the accuracy of computation results. Before flight tests, a ready-made UAV prototype is subject to ground resonance (modal) tests. These tests are conducted prior to final flutter computations.

Aerodynamic actions in subsonic and supersonic flight regimes are determined using different aerodynamic theories (typically – linear theories). Special-purpose software suites may be used for computations in the transonic flight envelope. In these flight conditions (at Mach numbers in the range of 0.95…105), the UAV flight safety regarding exposure to flutter can be assessed more accurately based on flight test results.

Below is the description of final computations. They are exemplified by the results, which provide correct assessment of the UAV flight safety regarding exposure to flutter. This paper supplements the information published in [3] with regard to ground tests.

Research sequence

A simplified variant of the research sequence for protecting the UAV against flutter includes several stages.

The first stage is intended to collect and normalize initial design data to comply with the selected software application.

The second stage is intended to develop a mathematical model of the UAV for preliminary computations of frequencies and modes of self-excited vibrations under no-flow conditions and for flutter computations.

The third stage is needed to conduct preliminary computations. The data is important for planning and conducting a ground experiment.

The fourth stage is an experimental study needed to determine characteristics of natural vibrations the full-scale UAV and its functioning systems are exposed to. This full-scale model is used for ground resonance (modal) tests.

At the fifth stage, a mass-elastic mathematical model is to be updated based on ground test results for final flutter computations.

The sixth stage is one of the most important stages. This stage is intended for final computations, the results of which are the rationale

for UAV safety assessment in any flight conditions.

The seventh and final stage is needed to run a data analysis and to draw a conclusion intended to prevent dangerous self-excited vibrations during flight tests. Sometimes, it is necessary to elaborate recommendations for UAV modifications in order to ensure standard stability margins in flight. In this case, all introduced modifications are subject to performance tests.

This paper represents computational data related to the sixth stage – final flutter computations.

Mass-elastic models and natural vibration computations

Based on the previous studies of a variety of UAV models, we collected initial data and developed a mathematical model of the aircraft's mass-elastic structure.

Final flutter computations were conducted for the test UAV featuring a typical aerodynamic configuration with medium-aspect ratio smooth wings and independent control surfaces. We considered different weights of the wing and fuel compartment. Flutter computations were conducted considering differences in rotational stiffness of control surfaces.

Experiment results prove that the UAV body characteristics are not symmetrical relative to the control surfaces. As a rule, a computational model does not represent these specific features.

The bulk of computations were completed using the Ritz polynomial method in the KS-M software environment [4]. Additional computations were conducted using the finite element method in the *MSC.Nastran* software environment [5]. Computations of natural vibration frequencies of a cantilevered wing (outer wing), symmetric (symmetry) and antisymmetric (antisymmetry) vibrations of the full-scale UAV model wings were carried out using the KS-M software. Table 1 compares natural frequencies with reference frequencies f_A, which are represented by antisymmetric vibration frequencies:

$$\frac{(f - f_A)}{f_A}.$$

Table 1

Wing natural frequency comparison results (%)

Mode of vibration	Outer wing	Symmetric vibrations
Wing first bending mode	–21	–19
Wing second bending mode	–5	2
Wing first torsion mode	–2	1

Comparison of natural frequencies of control surfaces designated as control surfaces 1 and 2 is given in Table 2 (in KS-M). Individually, frequency diversity is caused by the influence of the body weight. Natural frequencies are referred to partial frequencies:

$$(f - f_{\text{парц}})/f_{\text{парц}}.$$

Table 2

Natural frequencies of control surfaces (%)

Mode of vibration	Cantilevered control surface	Full-scale UAV vibrations	
		Symmetric	Antisymmetric
Rotation of the 1st control surface	–0.5	–0.4…–0.5	–0.5
Rotation of the 2nd control surface	–1.0	–0.8…–1.0	–0.8…–1.0
Bending of the 1st control surface	–8.0	–6…–8	–8
Bending of the 2nd control surface	–8.0	–5.5…–8.0	–7…–6

Partial frequencies are determined by values of rotational stiffness $K_{\text{вр}}$ or bending stiffness $K_{\text{изг}}$ and relevant moments of inertia I_Z and I_X. The control surface is assumed to be inelastic while the product of inertia is equal to zero. The rotation mode partial frequency is determined as $(2\pi f_{\text{парц}})^2 = K_{\text{вр}}/I_Z$, and the bending mode partial frequency is $(2\pi f_{\text{парц}})^2 = K_{\text{изг}}/I_X$. Based on results of frequency comparison, we may conclude that differences for rotation of the control surface do not exceed 1 %, and for bending – 8 %.

Aerodynamic models

Distributed aerodynamic forces acting on the aircraft surface in flight at vibrations are represented as a set of estimated concentrated forces applied at several points, the number of which reaches several thousands. These forces form an aerodynamic grid which is coupled with a computational mass-elastic model during a special interpolation procedure in order to provide an accurate mathematical model. The principles of generation of an aerodynamic model using the KS-M and *MSC.Nastran* software have much in common.

In this case, the linear thin-wing theory is applied. For computations, each lifting surface is divided into aerodynamic panels, the number of which is limited. Setting the Mach number within the range $M \approx 0.95\ldots1.05$ is not recommended for computations using the KS-M and *MSC.Nastran software.*

For computations of aerodynamic matrices for subsonic flight velocities, the KS-M software uses the discrete dipole method, and for subsonic flight velocities – the panel method with the number of aerodynamic panels not exceeding 1 000. The UAV is a system of flat lifting surfaces parallel to the oncoming flow velocity vector. The surfaces are divided into smaller triangular or trapezoidal panels. Meanwhile, the solutions are supposed to be accurate if the selected Mach and Strouhal numbers correspond to the resulted flutter speed and frequency.

For $M < 1$, the *MSC.Nastran* software used the dipole localization method (*DLM*), and for $M > 1$ – the constant pressure method (*CPM*).

In order to evaluate the influence of the cylindrical section of the body, flutter computations were conducted with an aerodynamic grid modelling not only the entire body ("full grid"), but also the forebody ("only nose section"). The influence of the forebody for different shapes of flutter and Mach numbers was determined using the KS-M software.

In particular, for the symmetric shape of wing flutter, exposure of the surfaces and the forebody to aerodynamic action did not actually lead to a change of the flutter critical speed and frequency; as for the antisymmetric shape, the critical speed decreased by 7 % to meet our predictions.

For the symmetric form of control surface flutter, the absence of aerodynamic action on the cylindrical section of the body resulted in a decrease in the critical speed by 6 %. It is supposed to be reasonable not to plot an aerodynamic grid on the cylindrical section of the body.

In the course of computations using the KS-M software, we set values of density, Mach number, and Strouhal number (Sh) for each mode and determined the flutter critical speed. Based on its value and flutter frequency, we set the Sh number corresponding to the resulted critical mode, and this value was the initial one for computations in the next approximation. Examples of iterations are shown in Fig. 1.

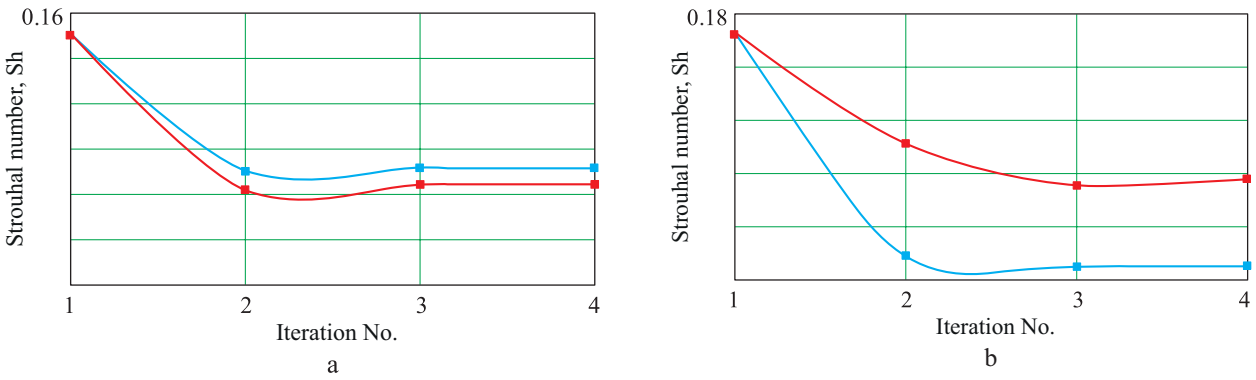

Fig. 1. Convergence by Strouhal numbers Sh for two shapes of flutter (a, b):
– symmetric model; – antisymmetric model

Wing flutter

Using the *MSC.Nastran* software, we conducted computations by changing flight speed $V = V_{min} \ldots V_{max}$ in a traditional way with interval ΔV at constant values of the M number and air density ρ ($p-k$) method). Design basis is 15 eigenmodes (with regard to solid body eigenmodes). During structural damping with the logarithmic decrement of 0.05 (relative damping coefficient $\zeta = 0.008$), M/M_0 numbers were equal to the following values: 0.9; 1.1; 1.2; 1.5; 1.7.

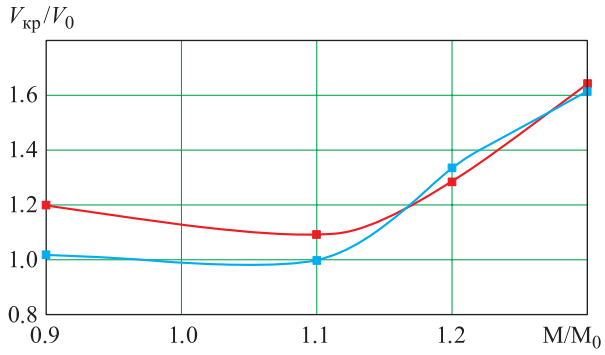

Fig. 2. Wing flutter critical speed
– symmetric model;
– antisymmetric model

Fig. 2 shows results of full-scale UAV flutter ("wing flutter") computations conducted by means of the KS-M. Design basis is 14 eigenmodes (with regard to solid body eigenmodes), with structural damping similar to the *MSC.Nastran* mathematical models. As the M number increases, critical flutter speed $V_{кр}$ increases accordingly, with substantial narrowing of differences between the symmetric and antisymmetric shapes of flutter.

Fig. 3 and Table 3 show changes in vibration frequency and damping on the root plane – relative damping coefficient ς and frequency *f* for the same shape of flutter which has already been computed using the *MSC.Nastran* software. Flight conditions correspond to various combinations of the M number and values of dimensionless altitude H/H_0. The parameter is the flight speed. In all circumstances, the higher the flight speed, the higher the vibration frequency. At $\varsigma = 0$, flutter can be observed only in the subsonic mode at the maximum density corresponding to $H/H_0 = 6$. There is a considerable speed margin exceeding the rated one.

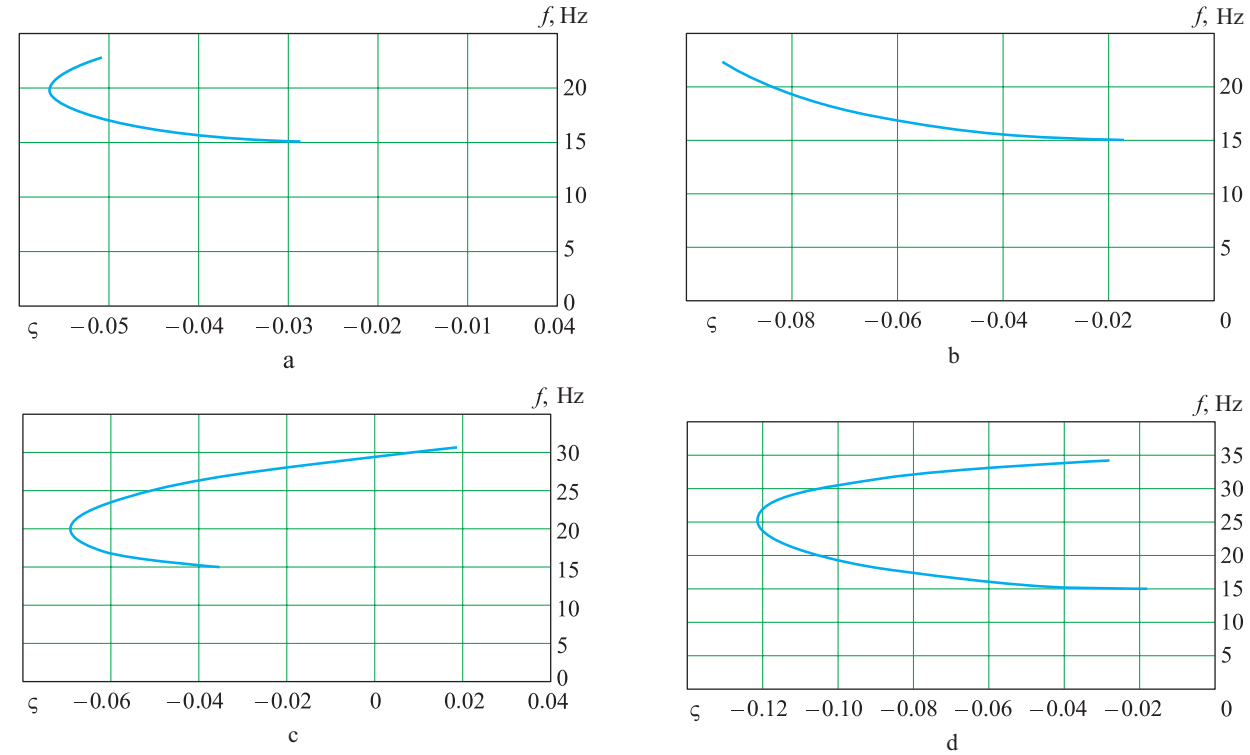

Fig. 3. Variation of frequency and damping on the root plane at the following combinations of relative altitudes and Mach numbers:
a – $H/H_0 = 10$, $M/M_0 = 1.1$; b – $H/H_0 = 10$, $M/M_0 = 0.9$;
c – $H/H_0 = 6$, $M/M_0 = 1.1$; d – $H/H_0 = 6$, $M/M_0 = 0.9$

Table 3

Wing flutter (antisymmetric model)

H / H_0	M / M_0	Typical frequency, Hz	Logarithmic decrement	$V_{кр}$, m/s	$f_{фл}$, Hz
10	1.1	17	0.25	> 650	> 34.4
10	0.9	16	0.13	> 650	> 22.4
6	1.1	18	0.19	630	29.5
6	0.9	17	0.22	> 650	> 34.4

The critical speed for the symmetric shape of wing flutter is lower by 8 % than that for the antisymmetric shape while the difference between flutter frequencies is 3 %. Proximity of stability limits can be caused by a considerable body weight when wing vibrations are loosely coupled and are near to vibrations of cantilevered wings. Table 4 specifies values $V_{кр}$ and $f_{фл}$ for variable total weight of the wing. Despite a considerable change of the weight (up to 1/2), the minimum critical speed varies within 6 %.

Besides, we conducted mathematical simulation of fuel burnout for the symmetric flutter shape and various fuel weights: total weight, half weight and zero weight. It is found out that a change of the body weight due to fuel burnout leads to considerably minor changes of the critical speed – up to 10 %, and to changes of flutter frequency – up to 6 %.

In order to understand the instability behaviour, sometimes it is vital to evaluate the contribution of individual modes to the onset of vibrations. Such evaluation can be done by the relative value of the vibration mode energy on the flutter boundary.

The KS-M software allowed to compute the ratios of vibration modes for wing flutter (Fig. 4). It is evident that the first three modes of vibration are the main ones with a minor contribution by the 4th mode.

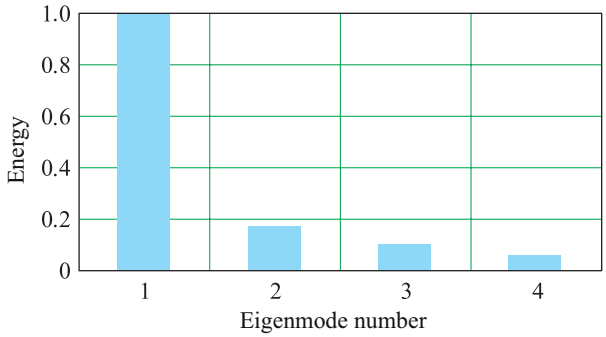

Fig. 4. Eigenmode energy at wing flutter: 1 – wing symmetric first bending mode; 2 – body first bending mode; 3 – control surface rotation; 4 – symmetric torsion of wing

The value of damping coefficient derivative δ depending on the flow velocity is also important. This value determines the flutter behaviour as well as the accuracy of boundary evaluation to a great extent. Error values are likely to be higher at a small value of the derivative and vice versa. Quantitative comparison of the damping coefficient derivative for wing flutter and control surface shape is given in Table 5. We should note that the derivative for outer wing flutter is two times higher in comparison with the shapes of wing flutter and body-control surface flutter. This indicates a more dramatic change of damping and self-excited vibration build-up. However, the flutter boundary can be identified more accurately at interference inherent to the experiment.

Table 5

Damping coefficient velocity derivative (at $V = V_{кр}$, KS-M)

Flutter shape	M / M_0	$d\delta$ / dv
Wing flutter shape	1.1	39
Control surface flutter shape flexural-torsional	1.2	58

Table 4

Values of flutter critical speed and frequency depending on the wing weight (symmetric model)

Wing	$V_{кр}$						$f_{фл}$					
	M / M_0						M / M_0					
	0.6	0.9	1.1	1.2	1.3	1.5	0.6	0.9	1.1	1.2	1.3	1.5
Light-weight	467	401	395	495	471	879	26.1	19.0	18.2	23.5	19.9	35.6
Rated	465	388	382	508	556	877	19.9	14.3	13.9	19.3	19.9	27.6
Heavy-weight	463	382	387	526	506	913	16.7	11.9	12.0	17.2	14.7	24.4

Controls flutter

Computations allowed to obtain the symmetric and antisymmetric shapes of controls flutter, to be more precise – body-control surface shapes. Fig. 5 shows hodographs on the root plane at $M / M_0 = 1.2$; similar markers and colour designate pairs of roots (eigenmodes) forming one of the flutter shapes. Fig. 6 shows dependencies of the critical speed of symmetric and antisymmetric shapes of control surface flutter on the M number at H = 0. Computations were performed using *MSC.Nastran*.

We should mention near values of the critical speed for two control surfaces, as well as convergence of frequencies of control surface vibration modes based on the root godograph at the fixed value of the M number. The same result is achieved when the M number changes, and critical speeds of symmetric vibrations of control surfaces nearly coincide when they are close to maximum values. According to experimental data, beating modes at very low frequencies and a transition from one flutter shape to the other with different ratios of control surface vibration amplitudes can be observed in such regimes or near them.

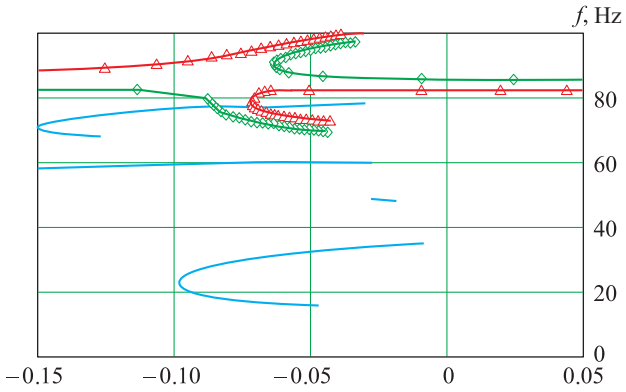

Fig. 5. Hodographs on root plane at $M/M_0 = 1.2$

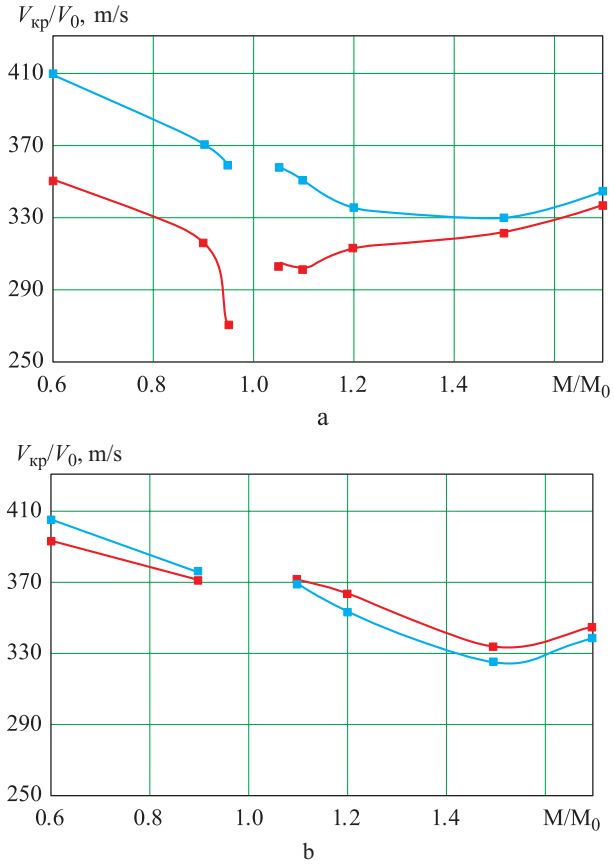

Fig. 6. Dependencies of critical speed $V_{кр}$ of symmetric (a) and antisymmetric (b) shapes of control surface flutter on the Mach number at $H = 0$: —■— – upper control surface; —■— – lower control surface

We should mention near values of the critical speed for two control surfaces, as well as convergence of frequencies of control surface vibration modes based on the root godograph at the fixed value of the M number. The same result is achieved when the M number changes, and critical speeds of symmetric vibrations of control surfaces nearly coincide when they are close to maximum values. According to experimental data, beating modes at very low frequencies and a transition from one flutter shape to

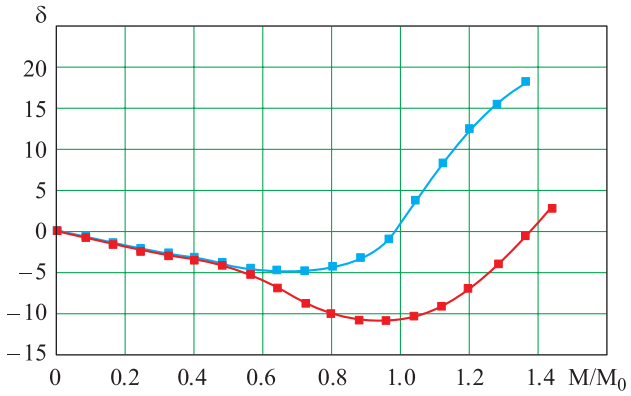

Fig. 7. Damping coefficient (real part of root) for flutter of 1st (—■—) and 2nd (—■—) control surfaces

Fig. 7 shows the dependence of the damping coefficient (real part of root) on the M number computed by means of the KS-M.

Natural frequencies of control surfaces under no-flow conditions were sufficiently close to each other, while in flow conditions they were different at the beginning as the speed increased (with the flutter boundaries sufficiently spaced); at the maximum speed frequencies converged again.

Using the KS-M software, we evaluated the contribution of individual vibration mode to forming of the body-control surface shape of flutter for one of the control surfaces. This evaluation is given in Table 6 as a dimensionless value of vibration mode energy on the flutter boundary.

Table 6

Energy of eigenmodes of the body-control surface flutter shape

Eigenmode				
M / M_0	Control surface first bending mode	Control surface rotation	Body first bending mode	Control surface second bending mode
1.2	1.0	0.30	0.12	0.17
1.5	1.0	0.26	0.03	0.02

According to data of Table 6, we may conclude that the energy of the body-control surface flutter shape is close to the energy of the cantilever shape of control surface flutter, which mainly depends on its first bending mode and rotation. Contribution of two other modes turns out to be relatively small.

Conclusion

We did parametric calculations for symmetric and antisymmetric flutter shapes of the wings and the tail.

Based on the results, we may conclude that there is a small difference between the critical speed of the cantilever shape of wing flutter and the shape of flutter of the symmetric wing model, while fuel burnout has an insignificant effect on flutter.

Control surface flutter shapes turned out to be the most dangerous. Small differences between partial frequencies of control surfaces result in forming of two shapes with close values of flutter critical speed. The study results will be helpful for a cycle of computations and research works intended to prevent dangerous self-excited vibrations in flight, in particular, the UAV flutter. *The study was conducted at the Central Aerohydrodynamic Institute named after N. E. Zhukovsky.*

Bibliography

1. Aerouprugost’ / *A. M. Matvienko, A. I. Akimov, M. G. Akopov* [i dr.] // Mashinostroenie. Entsiklopediya. T. IV–21. Samolety i vertolety. Kn. 1. Aerodinamika, dinamika poleta i prochnost’. M.: Mashinostroenie, 2002. S. 627–692. (Russian)

2. *Parafes’ S. G., Smyslov V. I.* Metody i sredstva obespecheniya aerouprugoy ustoichivosti bespilotnykh letatelnykh apparatov. M. Izd-vo MAI, 2013. 176 s. (Russian)

3. *Dolgopolov A. V., Leonteva R. V., Smyslov V. I.* Ground vibration tests of an unmanned aerial vehicle using multi-channel equipment // Journal of “Almaz – Antey” Air and Space Defence Corporation. 2016. No. 4. P. 72–80. (Russian)

4. *Bunkov V. G., Ishmuratov F. Z., Mosunov V. A.* Reshenie nekotorykh zadach aerouprugosti na osnove sovremennoi versii polinominal’nogo metoda Ritsa. Trudy TsAGI, Vyp. 2664, 2004. S. 97–116. (Russian)

5. MSC.Nastran Aeroelastic Analysis User’s Guide // SCRIBD. URL: https://ru.scribd.com/document/20953143/MSC-Nastran-Aeroelastic-Analysis-User-s-Guide (data access 20.05.2018).

Submitted on 02.04.2018

Mosunov Valeriy Arkad’evich – Candidate of Engineering Sciences, Senior Research Fellow, the Central Aerohydrodynamic Institute named after N. E. Zhukovsky, Zhukovsky.
Science research interests: dynamics and strength of aerial vehicles.

Ryabykina Regina Vladimirovna – Leading Engineer, the Central Aerohydrodynamic Institute named after N. E. Zhukovsky, Zhukovsky.
Science research interests: dynamics and strength of aerial vehicles.

Smyslov Vsevolod Igorevich – Doctor of Engineering Sciences, Chief Research Fellow, the Central Aerohydrodynamic Institute named after N. E. Zhukovsky, Zhukovsky.
Science research interests: dynamics and strength of aerial vehicles.

Frolov Aleksandr Vladimirovich – Candidate of Engineering Sciences, Leading Engineer, the Central Aerohydrodynamic Institute named after N. E. Zhukovsky, Zhukovsky.
Science research interests: dynamics and strength of aerial vehicles.

Опыт расчетных исследований флаттера беспилотного летательного аппарата

Рассмотрена последовательность расчетно-экспериментальных работ по флаттеру. Сформированы исходные данные образца беспилотного летательного аппарата, созданы математические модели. Проведены исполнительные параметрические расчеты симметричных и антисимметричных форм флаттера крыльев и оперения. Исследовано влияние аэродинамики на корпус летательного аппарата, приведены примеры результатов расчета по программным комплексам КС-М и *MSC.Nastran*.

Ключевые слова: флаттер, беспилотный летательный аппарат, расчетно-экспериментальные исследования, симметричная модель, антисимметричная модель.

Мосунов Валерий Аркадьевич – кандидат технических наук, старший научный сотрудник ФГУП «Центральный аэрогидродинамический институт имени профессора Н. Е. Жуковского», г. Жуковский.
Область научных интересов: динамика и прочность летательных аппаратов.

Рябыкина Регина Владимировна – ведущий инженер ФГУП «Центральный аэрогидродинамический институт имени профессора Н. Е. Жуковского», г. Жуковский.
Область научных интересов: динамика и прочность летательных аппаратов.

Смыслов Всеволод Игоревич – доктор технических наук, главный научный сотрудник ФГУП «Центральный аэрогидродинамический институт имени профессора Н. Е. Жуковского», г. Жуковский.
Область научных интересов: динамика и прочность летательных аппаратов.

Фролов Александр Владимирович – кандидат технических наук, ведущий инженер ФГУП «Центральный аэрогидродинамический институт имени профессора Н. Е. Жуковского», г. Жуковский.
Область научных интересов: динамика и прочность летательных аппаратов.